

Sustained high winter glacier velocities from brief warm events

Léo Decaux ¹, Kenneth D. Mankoff ^{2,3}, Mariusz Grabiec ¹, Andreas Alexander
⁴, Joanna Tuszynska ¹, Bartłomiej Luks ⁵ and Jacek Jania ¹

¹University of Silesia in Katowice, Faculty of Natural Sciences, Institute of Earth Sciences, Bedzinska 60,
41-200 Sosnowiec, Poland

²National Snow and Ice Data Center, University of Colorado, Boulder, CO 80309 USA

³Department of Glaciology and Climate, Geological Survey of Denmark and Greenland (GEUS), Øster
Voldgade 10, DK-1350, Copenhagen K, Denmark

⁴Department of Geosciences, University of Oslo, 0316 Oslo, Norway

⁵Institute of Geophysics, Polish Academy of Sciences, Ksiecia Janusza 64, 01-452 Warsaw, Poland

Key Points:

- A single week-long warm event in the winter can lead to a more than doubling of the velocity of the glacier for more than 3 months

Corresponding author: Léo Decaux, leodecaux@gmail.com

Abstract

A single week-long warm event in midwinter in Svalbard flooded an inefficient en- and subglacial drainage system and led to a 2.5x velocity increase that remained in effect for the remainder of the winter - more than 3 months. Because of the long winter season, changes in winter velocity have a large impact on the annual average velocity. As the climate warms and surface melt and rain events increase during winter months, sustained high winter glacier velocities are likely to occur more often. Increasing glacier velocity near the terminus leads to additional ice entering the fjord, and an increase of ice dynamics contribution to sea level rise during winter.

Plain Language Summary

Most glacial field studies occur in summer due to the difficulties of winter polar fieldwork. However, because of this long Arctic winter season, changes in the winter ice speed can cause large changes in annual average speed. The causes of these changes are generally well-understood and linked to water inputs to the inside and the base of the glacier. We installed a pressure transducer in an ice cave, and combined with a model, weather stations, and GPS measuring ice speed, we show that a single week-long warm event in the winter led to a more than doubling of the winter velocity for more than 3 months. In a warming climate, more winter melt and rain is likely to occur, and may lead to increased winter glacier velocity, additional ice entering fjords, and increased rates of sea level rise.

1 Introduction

Glacier velocity changes are primarily driven by internal drainage system (IDS) hydrologic changes (Anderson et al., 2004; Bingham et al., 2006; Brinkerhoff et al., 2016; Hooke et al., 1997; Iken & Bindenschadler, 1986; Jansson, 1995; Mair et al., 2003; Willis, 1995). In the spring, warming atmospheric temperatures start melting the glacier surface, and snowfall becomes rain. As the meltwater and rain enters an inefficient subglacial system, effective basal pressure decreases and ice velocity increases. Eventually, larger volumes of basal water carve large subglacial channels that efficiently exhaust the water, and a mid-to-late summer slowdown may occur. Minimum velocity is often in the early fall when the surface runoff stops and water leaves the subglacial system more quickly than the creep closure of the large subglacial conduits, leading to high effective pressure. Throughout the winter, velocity starts to increase again as subglacial conduits shrink and decrease the effective basal pressure. There may also be some delayed water from the upper part of the glacier that impacts winter velocity (Joughin et al., 2008; Stevens et al., 2016; Vijay et al., 2019).

Overlaid on the seasonal cycle, short-term velocity increases are generally associated with lake drainage, rain, or excessive warm events – all of which can generate sufficient surface meltwater that, when delivered to the bed, can temporarily overwhelm even large subglacial channels (Anderson et al., 2014; Bartholomaeus et al., 2008; Doyle et al., 2015; Hart et al., 2019; Schoof, 2010).

Because the IDS is less efficient in the winter or early spring, less water is needed in these seasons to fill it, overwhelm it, and cause an ice dynamics response. This property is the cause of spring velocity spikes observed on temperate and polythermal glaciers and ice sheets (Bingham et al., 2006; I. Hewitt, 2013; Kessler & Anderson, 2004; Mair et al., 2003), and why many surge events, correlated with high basal water pressures, start in winter (Harrison & Post, 2003; Kamb et al., 1985; Lingle & Fatland, 2003; Sund et al., 2014).

62 Although glacier studies usually occur during summer months, likely due to the
63 difficulties of Arctic winter fieldwork, there is an increasing body of literature highlight-
64 ing the importance of variability in winter motion (e.g., Burgess et al., 2013; Hart et al.,
65 2019; Schoof et al., 2014; Sole et al., 2013). Because the Arctic winter (and associated
66 slower glacier velocities) is longer than the Arctic summer (and associated glacier veloc-
67 ity increase), an increase in winter ice velocity can have a disproportionately large in-
68 crease in annual average ice velocity.

69 Here we add to the growing body of winter velocity studies by presenting a time
70 series of 2016 and 2017 winter observations at a polythermal high Arctic glacier. Data
71 include water level from inside an englacial channel, velocity measurements of the glacier
72 surface, automatic weather station (AWS) data, remote sensing synthetic aperture radar
73 (SAR) images of the glacier surface, and a regional short-range high-resolution weather
74 model.

75 2 Study area

76 Hansbreen is a 15.6 km long polythermal tidewater glacier, with a mean ice thick-
77 ness of 171 m (Grabiec et al., 2012), situated at 77° 04'N, 15° 38'E in southwest Spits-
78 bergen (Figure 1a). It flows towards the south, extending from 664 m altitude to sea level,
79 with a ca. 150 m yr⁻¹ velocity at the terminus and a 55–70 m yr⁻¹ velocity 3.7 km up-
80 stream (Błaszczuk et al., 2009). It is climatically, environmentally, and glaciologically
81 similar to other Svalbard tidewater glaciers (Grabiec et al., 2012; Hagen et al., 1993, 2003).
82 In the past, water level measurements have been collected directly from within its moulins
83 (Schroeder, 1998a, 2007; Vieli et al., 2004) indirectly via ground-penetrating radar (GPR)
84 (Jania et al., 2005), and there have been several en- and sub-glacial explorations quan-
85 tifying bed properties (Benn et al., 2009; Chen et al., 2018; Gulley et al., 2012, 2014; Mankoff
86 et al., 2017)

87 This study focuses on measurements from inside an englacial system called Crys-
88 tal Cave (CC, Figure 1), which has been active since at least 1967 (Benn et al., 2009;
89 Turu, 2012; Schroeder, 1998a, 1998b). Crystal Cave is know to recharge from four moulins
90 and may be occasionally supplied during high discharge events by one additional moulin
91 and one supraglacial stream (Figure 1b) flowing at the interface of the Tuva nunatak and
92 the Tuvbreen glacier (Figure 1a). A subglacial model shows the presence of a subglacial
93 channel nearby CC's entrance (Decaux et al., 2019) and GPR measurements confirm its
94 connection with the subglacial drainage network (Pälli et al., 2003).

95 3 Methods

96 3.1 Velocity

97 We measured velocity with a Global Navigation Satellite Systems (GNSS) receiver
98 Leica Geosystems GPS1200 (L1/L2), that sampled every 3 hours at stake 4MONIT (Fig-
99 ure 1a). Daily speed was calculated from daily displacement of the stake. We define the
100 baseline velocity as the mean velocity from December 1 2016 through February 1 2017.

101 The velocity has also been surveyed for decades at a stake network along Hansbreen's
102 center line (stakes 2 through 11 in Figure 1a) but with a lower temporal resolution. GNSS
103 positions were recorded (with the same receiver model as at stake 4MONIT) weekly for
104 stakes 2 through 5, and monthly for stakes 6 through 11, depending on weather condi-
105 tions. The minimum observation time at those stakes is between 20 and 30 minutes. Speed
106 is reported in meter per day even when measured over longer time periods.

107 Post-processing of all GNSS measurements is done at the Polish Polar Station with
108 Leica Geo Office software by using the reference station (Leica GRX1200 Pro) located

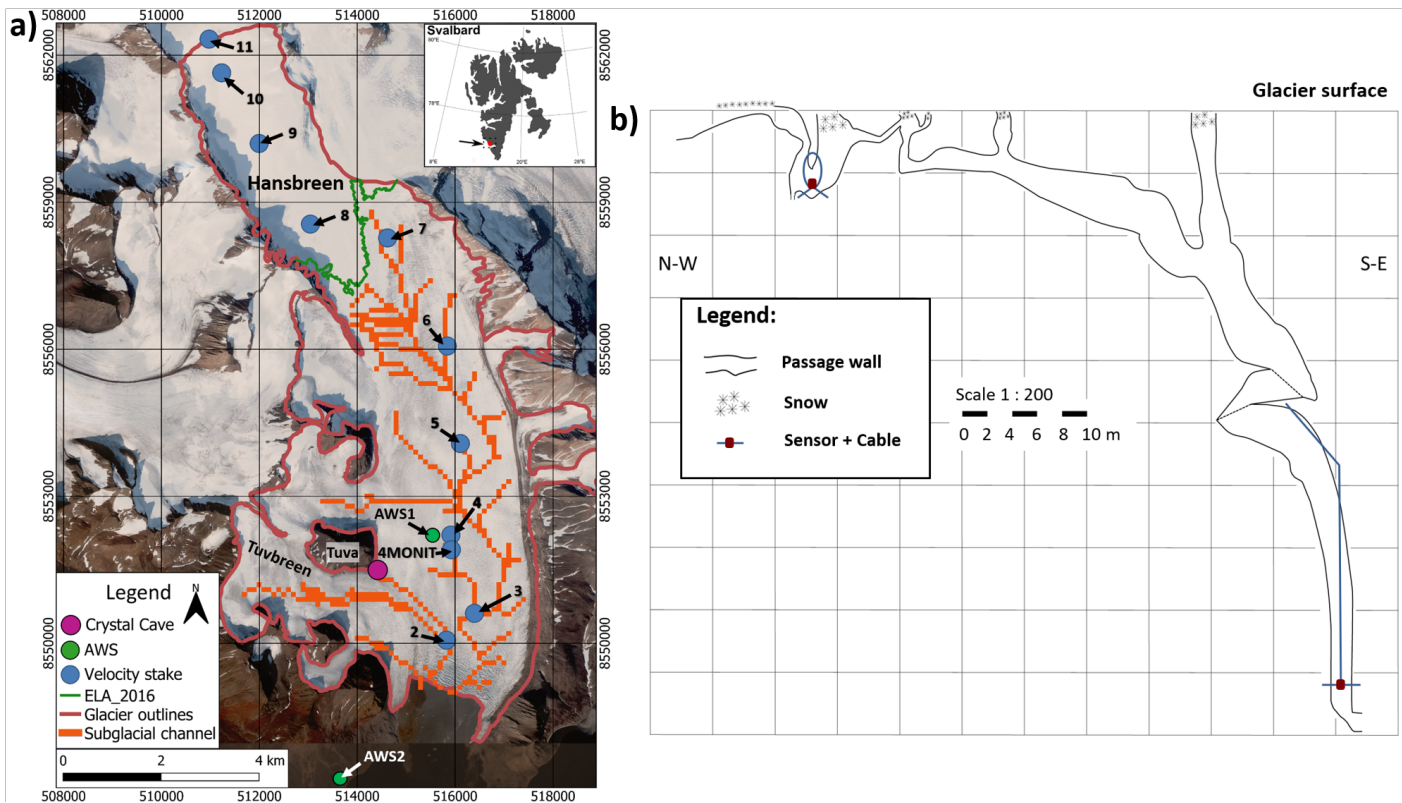


Figure 1. (a) Map showing the locations of the glacier Hansbreen in Svalbard (insert map), the two automatic weather stations (AWS), the 10 velocity stakes, Crystal Cave, subglacial channels from Decaux et al. (2019) and the ELA for 2016 (the accumulation area being above the ELA and ablation area being below the ELA). The background map is an WorldView-2 satellite image acquired on 21 August 2015 combined with an ASTER satellite image acquired on 17 August 2020 and the coordinate system used is WGS 1984 UTM zone 33N. (b) Vertical profile of englacial channel Crystal Cave from April 2017 with sensors locations.

109 at the Polish Polar Station. The estimated error is between $\pm 0.025 - 0.005 \text{ m day}^{-1}$ and
 110 is more than an order of magnitude lower than our measurements.

111 **3.2 Englacial water pressure**

112 Englacial water pressure was recorded by placing HOBO 250-Foot Depth Water
 113 Level Data Loggers inside the the Crystal Cave system (Figure 1b). Data loggers recorded
 114 pressure and temperature every 30 minutes, have a resolution of 2.55 kPa for a typical
 115 error of 3.8 cm water level, and were resampled to daily average values in post-processing.

116 Sensors were placed in vertical sections of the cave by drilling anchor points into
 117 the ice roof above the vertical shaft, then hanging cables down in the center of conduit
 118 (Figure 1b). Stabilization cables were used to keep sensors from attaching to and freez-
 119 ing into ice walls by attaching the sensor to three horizontal cables anchored into the ice
 120 walls at ca. 120 degrees apart. Although we installed two sensors in CC using this method,
 121 the upper one was quickly buried due to the cave surface melting down and drifting snow
 122 (Figure 1b).

123 Here, we report data from the lower sensor installed in CC 28 m above the glacier
 124 bed (measured) and 46 m below the ice surface (estimated) (Figure 1b) in ice estimated
 125 to be 74 m thick. We calculate the flotation fraction k as the ratio between water pres-
 126 sure (P_w) and ice overburden pressure (P_i) (Flowers & Clarke, 1999) following equation
 127 1 and 2:

$$k = \frac{P_w}{P_i}, \quad (1)$$

128 with:

$$P_w = \rho_w g z_w \quad \text{and} \quad P_i = \rho_i g z_i, \quad (2)$$

129 where ρ_w is the water density (1000 kg m^{-3}), ρ_i is the ice density (917 kg m^{-3}), g is the
 130 acceleration due to gravity (9.81 m s^{-2}), z_w and z_i are respectively water level above the
 131 bedrock (measured in the cave in m) and ice thickness (74 m).

132 3.3 Weather

133 3.3.1 Observed

134 A nearby weather station, 1.8 km away from CC, provides air temperature from
 135 the glacier surface at ca. 165 m a.s.l (AWS1 in Figure 1a). Air temperature, sampled
 136 every 10 minutes with $\pm 0.1^\circ \text{ C}$ accuracy, comes from a Campbell Scientific 107, and is
 137 averaged to daily resolution in post-processing. Precipitation measurements were made
 138 at AWS2 at ca. 10 m a.s.l (Figure 1a), located at the Polish Polar Station ca. 1.6 km
 139 from the glacier front, with a Hellmann rain gauge D-200 that measured both solid and
 140 liquid precipitation. Results were converted into liquid water equivalent in millimeters.
 141 Because the measurements are carried out at 0600 UTC+1, the precipitation day is de-
 142 fined as beginning at 0600 UTC+1 on the observed day and ending 0600 UTC+1 on the
 143 day after. Therefore, precipitation measurements are temporally offset by 6 hours.

144 3.3.2 Modeled

145 Meteorological data from the AROME-Arctic model were to provide a spatially broader
 146 view of weather events than can be provided by the point-measurements from the AWS.
 147 The AROME-Arctic model is a regional short-range high-resolution forecasting system
 148 for the European Arctic with a 2.5 km grid resolution developed by the Norwegian Me-
 149 teorological Institute (Køltzow et al., 2019; Müller et al., 2017). Forecasted surface vari-
 150 ables (e.g., 2 m temperature, 2 m humidity) are interpolated over the grid based on op-
 151 timal interpolation (Giard & Bazile, 2000). Alexander et al. (2020) validated the fore-
 152 casted weather with observed weather for the Svalbard airport for the observation pe-
 153 riods in 2016 and 2019. The airport observations show good agreement with the closest
 154 grid point of the model in the general trends of both air temperature and rainfall.
 155 Here we used hourly model data to calculate average daily temperature and net precip-
 156 itation. Because we present daily average results, it is possible to have liquid rain on a
 157 day when the daily average temperature is below zero.

158 3.4 Satellite data

159 In addition to point-observations of rain and warm events from the AWSs, and re-
 160 gional model results, we also show remotely sensed rain in synthetic aperture radar (SAR)
 161 data following methods from Winsvold et al. (2018). For the study period, Sentinel-1 A
 162 radar images (from orbit 37 with a repeat cycle of 12 days) were converted to radiomet-
 163 rically calibrated backscatter images. We applied a backscatter terrain correction using

164 the digital elevation model ASTER 1sec GDEM, and then converted the linear backscat-
 165 ter values to decibels (dB; Figure 3a-e).

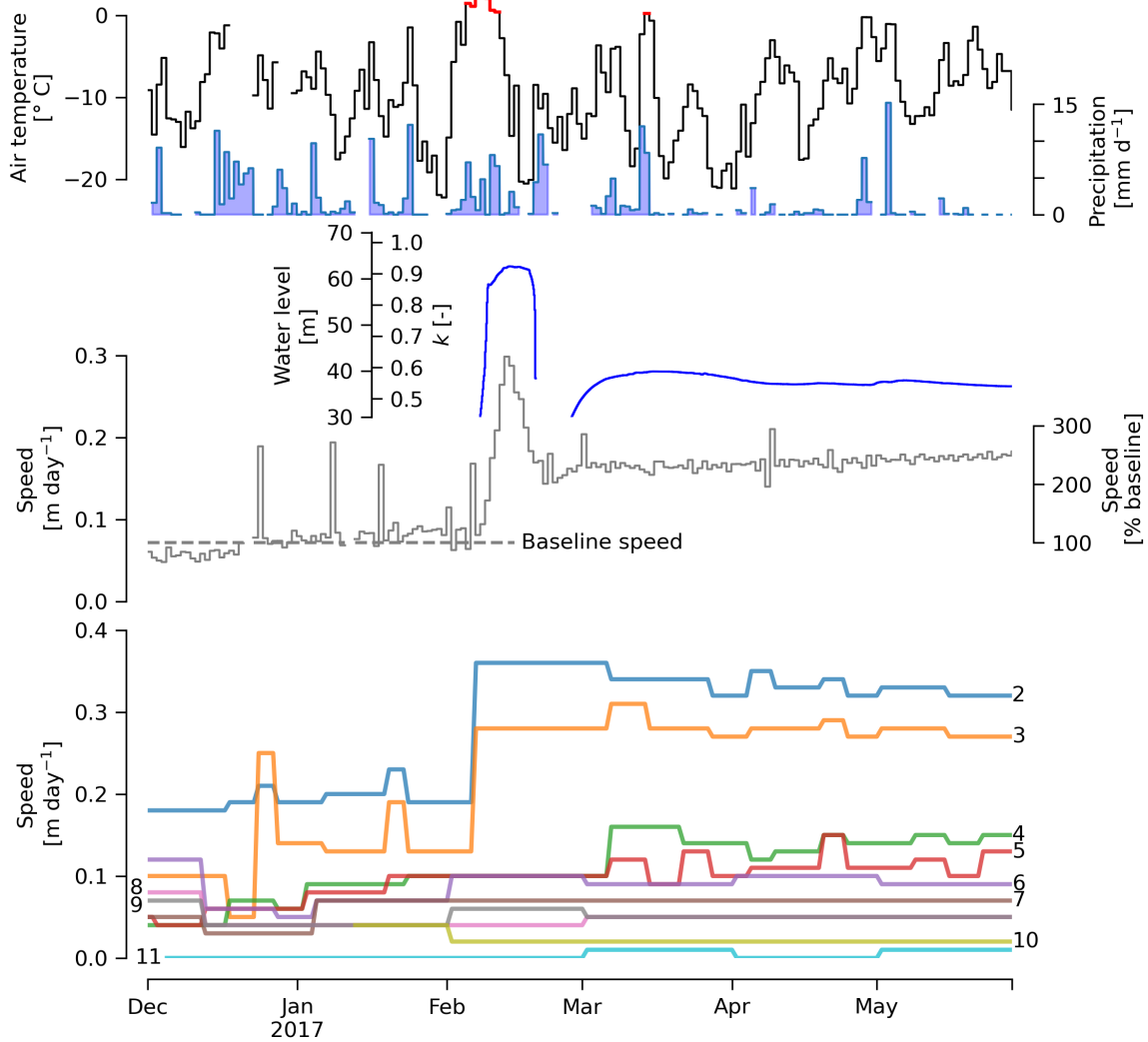


Figure 2. Time series of air temperature at AWS1 (positive red line and negative black line), precipitation (solid, mixed and liquid) at AWS2 (blue area), water level above the bedrock at CC and flotation fraction (k) (blue line) glacier speed at 4MONIT stake (grey line), and glacier speed at all other stakes (bottom panel) during the winter 2016/2017.

166 4 Results

167 During our study period, from 2016-12-01 through 2017-05-29, daily average tem-
 168 peratures recorded at AWS1 were below 0° C except for two periods, of which only one
 169 was longer than two days. From AWS2 and AROME-Arctic model, both of these warm
 170 events included rainfall events (Figures 2 and 3).

171 4.1 Temperature and hydrology

172 We highlight the week-long warm period (6 days 20 hours and 30 minutes) with
 173 a maximum of 3° C and mean of 1.5° C in early February 2017 (Figure 2). During this
 174 period, rain fell over the entire glacier surface (Figure 3). Prior to this warm event, the
 175 glacier surface is relatively dry (Figure 3a,b), and water level was below the sensor (less
 176 than 28 m above the bed) and therefore not shown in figure 2. On 16 February 2017,
 177 five days after the winter melt/rainfall event, the entire glacier surface is wetter (Fig-
 178 ure 3c). Beginning 64.5 hours after the first melt day (temperature > 0° C) water rose
 179 over 3 days to more than 60 m above the glacier bed, remained there for more than 9
 180 days, then rapidly dropped below the sensor for about 7 days, and returned to a level
 181 around 38 m above the bedrock (k around 0.55), and remained there for the duration
 182 of the record, until June 2017 (Figure 2). Several weeks after the warm event, the glacier
 183 surface is drier (Figure 3d, e).

184 4.2 Velocity

185 The velocity record at 4MONIT begins at ca. 0.07 m day⁻¹ and climbs slowly to
 186 just under 0.1 m day⁻¹ from 1 December 2016 through 10 February 2017. Coincident
 187 with the water level increase, velocity increased to more than 400 % of the baseline ve-
 188 locity, then dropped to ca. 200 % and then remained near 250 % of the baseline veloc-
 189 ity for the duration of the record, until June 2017.

190 The lower ablation area of the glacier (stakes 2 through 4) reacted similarly to stake
 191 4MONIT (Figure 2). The upper ablation area (stakes 5 through 7) also exhibited an in-
 192 crease in average winter velocity after the warm event. The accumulation area (stakes
 193 8 to 11) did not respond to the event (Figure 2).

194 5 Discussion

195 Because of the length of Arctic winter vs. summer the annual velocity is primar-
 196 ily controlled by the winter velocity (Table 1). Therefore, persistent high winter veloc-
 197 ities represent a substantial dynamic response and potential significant source of addi-
 198 tional sea level rise. The occurrence of winter warm events (Pitcher et al., 2020; Wu, 2017)
 199 and winter rain events (Nowak & Hodson, 2013) in the Arctic is increasing (Graham et
 200 al., 2017; Lupikasza et al., 2019; Moore, 2016; Peeters et al., 2019; Sobota et al., 2020;
 201 Vikhamar-Schuler et al., 2016). Winter warm events may have a larger influence on the
 202 annual average velocity of the glacier than a warm event or a rain event in summer - in
 203 the case presented here, a brief winter warm event increased glacier velocity more than
 204 200 % over the baseline velocity for several months. Until enough winter water enters
 205 the glacier system to cause efficient drainage channels, it is likely that small volumes of
 206 winter water, spread over the entire glacier, will act analogous to a "spring event", in-
 207 ducing an increase in ice velocity (Bingham et al., 2006; Kessler & Anderson, 2004; Mair
 208 et al., 2003), with no subsequent decrease, as shown here. This persistent doubling ve-
 209 locity from the baseline only occurs in the ablation area (Figure 2), as the IDS does not
 210 exist in the accumulation area (Decaux et al., 2019).

211 The winter warm event described here supplied the entire glacier with a both melt-
 212 water and rain (Figure 2 and 3) resulting in wetting of the entire glacier surface (Fig-
 213 ure 3c). We are not able to determine using the SAR images if the lowermost part of Hans-
 214 breen has been influenced by this event (Figure 3c) due to crevasses causing an increase
 215 in backscatter coefficient (Forster et al., 1996). After the warm event and coincident rise
 216 in water level (Figure 2), the water briefly drops below the sensor (< 28 m above the bed),
 217 then returns to 38 m above the bed, followed by a slight decrease in water level and slight
 218 increase in velocity. We hypothesize that the volume of meltwater generated by the warm
 219 event was large enough to briefly reopen the IDS. If so, then some water likely evacu-

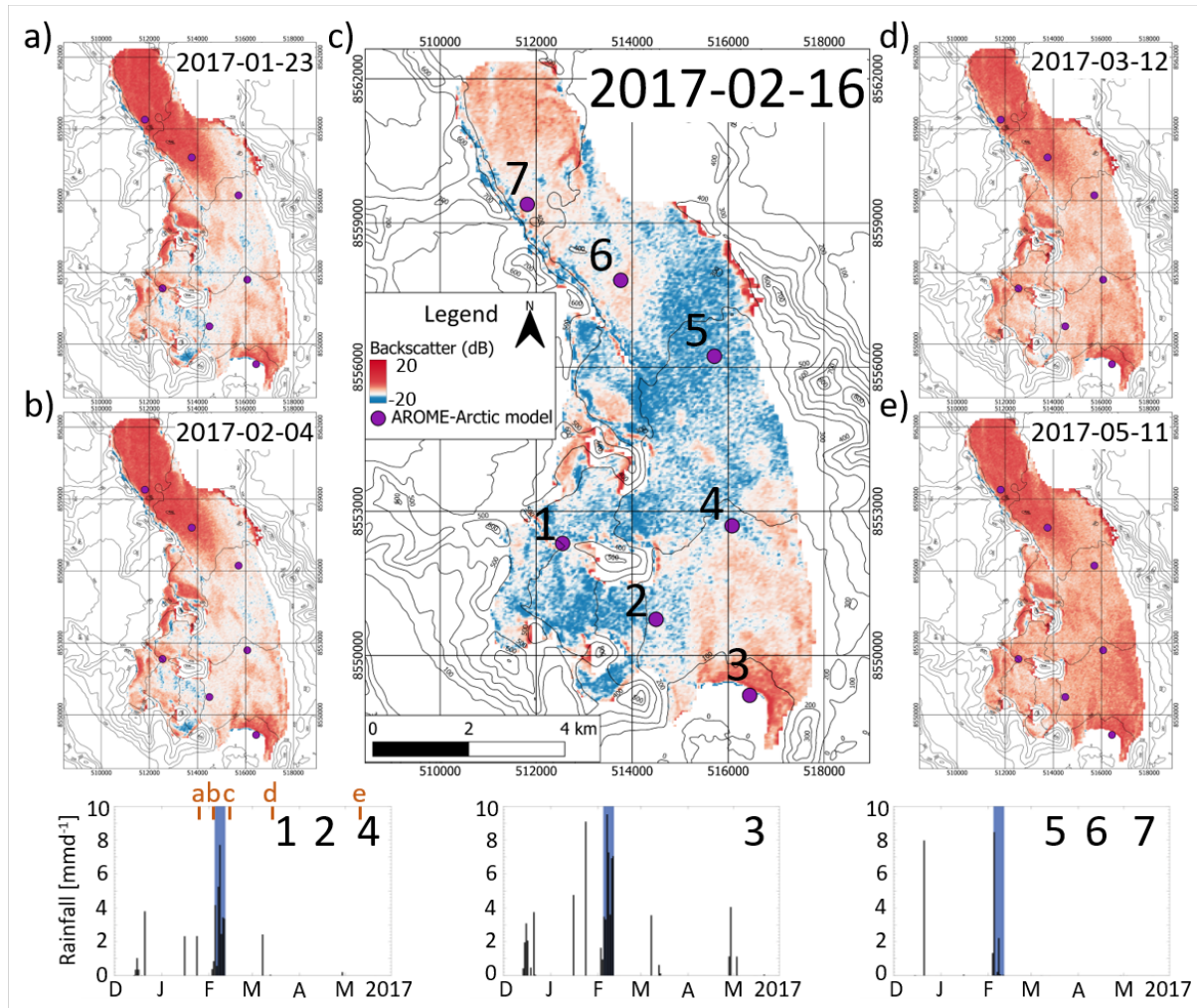


Figure 3. Sentinel-1A backscatter (dB) images from five different days for Hansbreen (a-e). Blue color indicates lower backscatter values showing wetter conditions. The three graphics represent the rainfall modeled by the AROME-Arctic model for seven locations shown on the map (c) by the corresponding numbered purple points for the study period. Winter melt event studied is highlighted in blue on each time series and images (a-e) are placed on the timeline of the first panel.

	Stake 3	Stake 4	Stake 5
Annual (2009-18)	0.37	0.21	0.15
Winter (2009-18)	0.36	0.20	0.15
Summer (2009-18)	0.40	0.22	0.17

Table 1. 10 years average velocity for stakes 3, 4 and 5 in m.d-1. Winter represents the period from October to May and summer the period from June to September.

220
221

ated out the glacier front, after which the remaining water was captured within in the IDS due to creep-closure of subglacial channels (Duval, 1977; Duval et al., 1983; Glen,

1955). It is likely creep closure explains the 10 m water level increase (from the sensor at 28 m above the bed to the final ca. 38 m above the bed; Figure 2) observed at the end of February. This upwelling, together with a re-pressurisation of the subglacial system, explains the velocity increases (Davison et al., 2019). After this upwelling ends in early March, the slow decrease in water level is due to water leaving this cave system. It is not likely that water is directly draining out the front of the glacier into the fjord, because a decrease in subglacial water volume would likely cause a decrease in ice velocity, not an increase as shown here. Therefore, the local decrease in water level is likely due to creep closure of the system, pushing water to the surrounding bed, and decreasing the effective pressure (Cowton et al., 2016; I. J. Hewitt, 2011; Werder et al., 2013), after which it may or may not leave the glacier. Water transfer from a channelized system to the surrounding bed increases the water pressure within the distributed system at the base of the glacier, leading to an increase in ice velocity (Cowton et al., 2016; Mair et al., 2002). This warm winter event may have also influenced the velocity of the following 2017 summer, which had an average near-terminus velocity 18 % higher than the last 10 years (0.47 m.d^{-1} compare to 0.40 m.d^{-1}) (Table 1).

If we assume stake 2 as representative of the front velocity (Figure 1a), its winter baseline velocity (from 2016-12-01 to 2017-02-01) is ca. 0.19 m day^{-1} . After the warm winter event its average velocity is ca. 0.34 m day^{-1} until the end of the accumulation season (end of May). The velocity increase from this warm event, lasting more than 3 months, is ca. 0.15 m day^{-1} . If the ice front did not move and velocity can be directly related to calving, then 80 % more ice entered the fjord in the 2016/2017 winter than if this 1-week warm event had not occurred, or ca. 20 % (ca. 5 Mt) more ice compared to the annual average. Here the annual increase is only 20 % from the 80 % winter increase, because the anomaly only occurs for 3 winter months.

Data gaps and velocity spikes - We show two gaps in the temperature record (duration of 6 days and 5 days), due to a sensor malfunction, during which precipitation events occur in December 2016 (Figure 2). There is no observed water level fluctuations (water level remained within 28 m of the bed) and no coincident velocity increase. Therefore, we assume that temperatures remain below 0° C . In addition, there are 3 one-day-long velocity increases prior to the February event, with coincident AROME-Arctic model rain events (Figure 3). We assume the cause of these short-term velocity increases is from these rain events. However, they have no lasting impact observed in our data.

Our dataset also highlights winter water storage with implications for observed winter discharge (e.g., Hodge, 1974; Hodgkins, 1997; Hodson et al., 2005; Jansson et al., 2003; Wadham et al., 2000). Our observed water level remains more or less steady at 38 m above the bedrock with k values around 0.55 (Figure 2), providing evidence of multi-month storage of large volumes of water. However, water can move dynamically and discharge to the distributed system, from the channelized one, while appearing more or less steady at the location of the logger, if the subglacial system closes equal to the volume discharged. We note that Pitcher et al. (2020) attribute their winter Greenland glacier discharge to storage of summer runoff, but acknowledge a warm event 10 days prior to their one day observation. Our data suggests that winter warm events may fill the system and could be the cause of winter discharge.

Similarly, Vijay et al. (2019) identified “type-3” glaciers in Greenland which are characterized by winter speedup events associated with subglacial meltwater activity. They assign the meltwater to different sources: basal meltwater, ocean water infiltrating into the subglacial system, and meltwater that did not evacuate through channels during the melt season and was retained in the firn and ice body. We suggest that in addition to these sources, winter warm events of which there are an increasing number in Greenland (Oltmanns et al., 2019), may create “type-3” glaciers.

273 The observations here are not unique to this glacier or Svalbard. After a warm win-
274 ter event in Iceland, a Glacsweb wireless probe installed at the Skálafellsjökull glacier
275 bed by Hart et al. (2019) observed a similar water pressure pattern. After an initial wa-
276 ter pressure increase attributed to the warm winter event, they recorded a sharp water
277 pressure decline followed by a slow rise on subsequent days until the next melt event (Hart
278 et al., 2019). Other Arctic glaciers may also be susceptible to these events. As the cli-
279 mate warms, precipitation onto the Greenland ice sheet is likely to shift towards a higher
280 fraction of rain in the total precipitation (Bintanja & Andry, 2017; Boisvert et al., 2018;
281 Lenaerts et al., 2020; Screen & Simmonds, 2012). If glacier dynamics models do not take
282 into account the increase in off-season rain shown by regional climate models, then they
283 may not properly model the magnitude of dynamic changes, with related limitations in
284 their ability to properly estimate sea level rise.

285 6 Conclusions

286 We show an Arctic glacier, as a result of a single week-long winter warm event, has
287 its average winter velocity in the ablation area more than quadruple (temporarily) and
288 remain at more than double the baseline for the remainder of the winter. The velocity
289 increase appears to be sustained by englacial and subglacial water storage. Within 10
290 days of the event a nearly steady state is reached, albeit with a small decrease in water
291 level and continued small increase in ice velocity for the remainder of the winter. We at-
292 tribute this to water transfer out of subglacial conduits to the distributed system at the
293 base of the glacier.

294 Warm winter events in the Arctic are being reported more often, and predicted to
295 occur more often in a warming climate. We show these warm events can lead to large
296 and sustained increases in ice velocity. Arctic tidewater glaciers are currently the most
297 significant contributor to eustatic sea level rise. Further studies linking the atmosphere,
298 ice velocity, and the winter subglacial hydrologic system are needed to quantify this con-
299 tribution to sea level rise.

300 Acknowledgments

301 Data Availability Statement

302 All the data are archived at the Polish Polar Data Base: [http://ppdb.us.edu.pl/
303 geonetwork/srv/eng/catalog.search#/home](http://ppdb.us.edu.pl/geonetwork/srv/eng/catalog.search#/home). Velocity data of 4MONIT stake and of
304 the center line of Hansbreen are respectively available at [http://ppdb.us.edu.pl/geonetwork/
305 srv/eng/catalog.search#/metadata/6e8f320d-4c06-40ce-86cc-f8561d3df4bb](http://ppdb.us.edu.pl/geonetwork/srv/eng/catalog.search#/metadata/6e8f320d-4c06-40ce-86cc-f8561d3df4bb) and
306 [http://ppdb.us.edu.pl/geonetwork/srv/eng/catalog.search#/metadata/8c5219c5
307 -2adb-40a5-a9de-eedcf8d0c7da](http://ppdb.us.edu.pl/geonetwork/srv/eng/catalog.search#/metadata/8c5219c5-2adb-40a5-a9de-eedcf8d0c7da). Air temperature and precipitation are respectively
308 available at [http://ppdb.us.edu.pl/geonetwork/srv/eng/catalog.search#/metadata/
309 e5e66a63-126d-49e1-bebe-c623becfb5d8](http://ppdb.us.edu.pl/geonetwork/srv/eng/catalog.search#/metadata/e5e66a63-126d-49e1-bebe-c623becfb5d8) and [http://ppdb.us.edu.pl/geonetwork/
310 srv/eng/catalog.search#/metadata/6603c86f-3194-4fbd-a7e8-5c0bbf430c94](http://ppdb.us.edu.pl/geonetwork/srv/eng/catalog.search#/metadata/6603c86f-3194-4fbd-a7e8-5c0bbf430c94). Wa-
311 ter level data of C.C are available at [http://ppdb.us.edu.pl/geonetwork/srv/eng/
312 catalog.search#/metadata/0a4570d3-576b-45e7-947e-737f610d976f](http://ppdb.us.edu.pl/geonetwork/srv/eng/catalog.search#/metadata/0a4570d3-576b-45e7-947e-737f610d976f).

313 This work has been financed by the Centre for Polar Studies, University of Sile-
314 sia – the Leading National Research Centre (KNOW) in Earth Sciences (2014–2018), No.
315 03/KNOW2/2014. Glaciological, hydrological and meteorological data were processed
316 by the University of Silesia data repository within project Integrated Arctic Observing
317 System (INTAROS). This project has received funding from the European Union’s Hori-
318 zon 2020 research and innovation programme under grant agreement no. 727890. Instru-
319 mentation was funded by the National Geographic Committee for Research and Explo-
320 ration Grant 9768-15. We wish to thank colleagues from the Polish Polar Station at Horn-
321 sund and the Institute of Geophysics Polish Academy of Sciences for hospitality and lo-

gistic support during field missions. Access to the meteorological data from the Hornsund station and GNSS data provided by the Institute of Geophysics, Polish Academy of Sciences is kindly acknowledged. The study used equipment and logistical resources belonging to the Polar Laboratory of the University of Silesia in Katowice. Thanks to the VENDYS foundation for its support. Thanks to Barbara Barzycka for providing data on ELA. Léo Decaux acknowledges the field assistance of Anton Sedlák, Kacper Konior, Jakub Medrzycki, Andreas Alexander, Konrad Osienienko, Sabina Kucieba, Kamil Pałkowski, Mateusz Mandat, Mariusz Czarnul, Maciej Błaszowski, Robert Pogorzelski, Dominika Dabrowska, Grzegorz Piotrowski, Benita Siepiera, Jakub Szewczyk, Bartosz Siek and Lukasz Pawłowski. There are no conflicts of interest.

References

- Alexander, A., Obu, J., Schuler, T. V., Kääb, A., & Christiansen, H. H. (2020). Subglacial permafrost dynamics and erosion inside subglacial channels driven by surface events in svalbard. *The Cryosphere*, *14*(11), 4217–4231.
- Anderson, Anderson, S. P., MacGregor, K. R., Waddington, E. D., O’Neil, S., Riihimaki, C. A., & Loso, M. G. (2004). Strong feedbacks between hydrology and sliding of a small alpine glacier. *Journal of Geophysical Research: Earth Surface*, *109*(F3).
- Anderson, Willis, I., Goodsell, B., Banwell, A., Owens, I., Mackintosh, A., & Lawson, W. (2014). Annual to daily ice velocity and water pressure variations on ka roimata o hine hukatere (franz josef glacier), new zealand. *Arctic, Antarctic, and Alpine Research*, *46*(4), 919–932.
- Bartholomäus, T. C., Anderson, R. S., & Anderson, S. P. (2008). Response of glacier basal motion to transient water storage. *Nature Geoscience*, *1*(1), 33–37.
- Benn, D., Gulley, J., Luckman, A., Adamek, A., & Glowacki, P. S. (2009). Englacial drainage systems formed by hydrologically driven crevasse propagation. *Journal of Glaciology*, *55*(191), 513–523.
- Bingham, R. G., Nienow, P. W., Sharp, M. J., & Copland, L. (2006). Hydrology and dynamics of a polythermal (mostly cold) high arctic glacier. *Earth Surface Processes and Landforms: The Journal of the British Geomorphological Research Group*, *31*(12), 1463–1479.
- Bintanja, R., & Andry, O. (2017). Towards a rain-dominated arctic. *Nature Climate Change*, *7*(4), 263–267.
- Błaszczyk, M., Jania, J. A., & Hagen, J. O. (2009). Tidewater glaciers of svalbard: Recent changes and estimates of calving fluxes. *Polish Polar Research*, *30*(2), 85–142.
- Boisvert, L. N., Webster, M. A., Petty, A. A., Markus, T., Bromwich, D. H., & Cullather, R. I. (2018). Intercomparison of precipitation estimates over the arctic ocean and its peripheral seas from reanalyses. *Journal of Climate*, *31*(20), 8441–8462.
- Brinkerhoff, D. J., Meyer, C. R., Bueler, E., Truffer, M., & Bartholomäus, T. C. (2016). Inversion of a glacier hydrology model. *Annals of Glaciology*, *57*(72), 84–95.
- Burgess, E. W., Larsen, C. F., & Forster, R. R. (2013). Summer melt regulates winter glacier flow speeds throughout alaska. *Geophysical Research Letters*, *40*(23), 6160–6164.
- Chen, Y., Liu, X., Gulley, J. D., & Mankoff, K. D. (2018, 10). Subglacial conduit roughness: Insights from computational fluid dynamics models. *Geophysical Research Letters*, *45*(20), 11,206–11,218. doi: 10.1029/2018gl079590
- Cowton, T., Nienow, P., Sole, A., Bartholomew, I., & Mair, D. (2016). Variability in ice motion at a land-terminating greenlandic outlet glacier: the role of channelized and distributed drainage systems. *Journal of Glaciology*, *62*(233), 451–466.

- 375 Davison, B. J., Sole, A. J., Livingstone, S. J., Cowton, T. R., & Nienow, P. W.
 376 (2019). The influence of hydrology on the dynamics of land-terminating sectors
 377 of the greenland ice sheet. *Frontiers in Earth Science*, 7, 10.
- 378 Decaux, L., Grabiec, M., Ignatiuk, D., & Jania, J. (2019). Role of discrete water
 379 recharge from supraglacial drainage systems in modeling patterns of subglacial
 380 conduits in svalbard glaciers. *The Cryosphere*, 13(3), 735–752.
- 381 Doyle, S. H., Hubbard, A., Van De Wal, R. S., Box, J. E., Van As, D., Scharrer, K.,
 382 ... Hubbard, B. (2015). Amplified melt and flow of the greenland ice sheet
 383 driven by late-summer cyclonic rainfall. *Nature Geoscience*, 8(8), 647–653.
- 384 Duval, P. (1977). The role of the water content on the creep rate of polycrystalline
 385 ice. *IAHS Publ*, 118, 29–33.
- 386 Duval, P., Ashby, M., & Anderman, I. (1983). Rate-controlling processes in the
 387 creep of polycrystalline ice. *The Journal of Physical Chemistry*, 87(21), 4066–
 388 4074.
- 389 Flowers, G. E., & Clarke, G. K. (1999). Surface and bed topography of trapridge
 390 glacier, yukon territory, canada: digital elevation models and derived hydraulic
 391 geometry. *Journal of Glaciology*, 45(149), 165–174.
- 392 Forster, R. R., Isacks, B. L., & Das, S. B. (1996). Shuttle imaging radar (sir-c/x-
 393 sar) reveals near-surface properties of the south patagonian icefield. *Journal of*
 394 *Geophysical Research: Planets*, 101(E10), 23169–23180.
- 395 Giard, D., & Bazile, E. (2000). Implementation of a new assimilation scheme for soil
 396 and surface variables in a global nwp model. *Monthly weather review*, 128(4),
 397 997–1015.
- 398 Glen, J. W. (1955). The creep of polycrystalline ice. *Proceedings of the Royal So-*
 399 *ciety of London. Series A. Mathematical and Physical Sciences*, 228(1175),
 400 519–538.
- 401 Grabiec, M., Jania, J., Puczko, D., Kolondra, L., & Budzik, T. (2012). Surface and
 402 bed morphology of hansbreen, a tidewater glacier in spitsbergen. *Polish Polar*
 403 *Research*, 33(2), 111–138.
- 404 Graham, R. M., Cohen, L., Petty, A. A., Boisvert, L. N., Rinke, A., Hudson, S. R.,
 405 ... Granskog, M. A. (2017). Increasing frequency and duration of arctic winter
 406 warming events. *Geophysical Research Letters*, 44(13), 6974–6983.
- 407 Gulley, J. D., Grabiec, M., Martin, J. B., Jania, J., Catania, G. A., & Głowacki, P.
 408 (2012). The effect of discrete recharge by moulins and heterogeneity in flow-
 409 path efficiency at glacier beds on subglacial hydrology. *Journal of Glaciology*,
 410 58(211), 926 – 940. doi: 10.3189/2012JoG11J189
- 411 Gulley, J. D., Spellman, P. D., Covington, M. D., Martin, J. B., Benn, D. I., &
 412 Catania, G. A. (2014). Large values of hydraulic roughness in subglacial
 413 conduits during conduit enlargement: Implications for modeling conduit
 414 evolution. *Earth Surface Processes and Landforms*, 39(3), 296–310. doi:
 415 10.1002/esp.3447
- 416 Hagen, J. O., Kohler, J., Melvold, K., & Winther, J.-G. (2003). Glaciers in svalbard:
 417 mass balance, runoff and freshwater flux. *Polar Research*, 22(2), 145–159.
- 418 Hagen, J. O., Liestøl, O., Roland, E., & Jørgensen, T. (1993). *Glacier atlas of sval-*
 419 *bard and jan mayen*. Norsk Polarinstitut Oslo.
- 420 Harrison, W. D., & Post, A. S. (2003). How much do we really know about glacier
 421 surging? *Annals of glaciology*, 36, 1–6.
- 422 Hart, J. K., Martinez, K., Basford, P. J., Clayton, A. I., Robson, B. A., & Young,
 423 D. S. (2019). Surface melt driven summer diurnal and winter multi-day stick-
 424 slip motion and till sedimentology. *Nature communications*, 10(1), 1–11.
- 425 Hewitt, I. (2013). Seasonal changes in ice sheet motion due to melt water lubrica-
 426 tion. *Earth and Planetary Science Letters*, 371, 16–25.
- 427 Hewitt, I. J. (2011). Modelling distributed and channelized subglacial drainage: the
 428 spacing of channels. *Journal of Glaciology*, 57(202), 302–314.

- 429 Hodge, S. M. (1974). Variations in the sliding of a temperate glacier. *Journal of*
 430 *Glaciology*, *13*(69), 349–369.
- 431 Hodgkins, R. (1997). Glacier hydrology in svalbard, norwegian high arctic. *Quater-*
 432 *nary Science Reviews*, *16*(9), 957–973.
- 433 Hodson, A., Kohler, J., Brinkhaus, M., & Wynn, P. (2005). Multi-year water and
 434 surface energy budget of a high-latitude polythermal glacier: evidence for over-
 435 winter water storage in a dynamic subglacial reservoir. *Annals of Glaciology*,
 436 *42*, 42–46.
- 437 Hooke, R. L., Hanson, B., Iverson, N. R., Jansson, P., & Fischer, U. H. (1997). Rhe-
 438 ology of till beneath storglaciären, sweden. *Journal of Glaciology*, *43*(143),
 439 172–179.
- 440 Iken, A., & Bindschadler, R. A. (1986). Combined measurements of subglacial wa-
 441 ter pressure and surface velocity of findelengletscher, switzerland: conclusions
 442 about drainage system and sliding mechanism. *Journal of Glaciology*, *32*(110),
 443 101–119.
- 444 Jania, J., Macheret, Y. Y., Navarro, F., Glazovsky, A., Vasilenko, E., Lapazaran, J.,
 445 ... Piwowar, B. (2005). Temporal changes in the radiophysical properties of a
 446 polythermal glacier in spitsbergen. *Annals of Glaciology*, *42*, 125–134.
- 447 Jansson, P. (1995). Water pressure and basal sliding on storglaciären, northern swe-
 448 den. *Journal of Glaciology*, *41*(138), 232–240.
- 449 Jansson, P., Hock, R., & Schneider, T. (2003). The concept of glacier storage: a re-
 450 view. *Journal of Hydrology*, *282*(1-4), 116–129.
- 451 Joughin, I., Das, S. B., King, M. A., Smith, B. E., Howat, I. M., & Moon, T. (2008).
 452 Seasonal speedup along the western flank of the greenland ice sheet. *Science*,
 453 *320*(5877), 781–783.
- 454 Kamb, B., Raymond, C., Harrison, W., Engelhardt, H., Echelmeyer, K., Humphrey,
 455 N., ... Pfeffer, T. (1985). Glacier surge mechanism: 1982-1983 surge of varie-
 456 gated glacier, alaska. *Science*, *227*(4686), 469–479.
- 457 Kessler, M. A., & Anderson, R. S. (2004). Testing a numerical glacial hydrological
 458 model using spring speed-up events and outburst floods. *Geophysical Research*
 459 *Letters*, *31*(18).
- 460 Køltzow, M., Casati, B., Bazile, E., Haiden, T., & Valkonen, T. (2019). An nwp
 461 model intercomparison of surface weather parameters in the european arctic
 462 during the year of polar prediction special observing period northern hemi-
 463 sphere 1. *Weather and Forecasting*, *34*(4), 959–983.
- 464 Lenaerts, J., Camron, M. D., Wyburn-Powell, C. R., & Kay, J. E. (2020). Present-
 465 day and future greenland ice sheet precipitation frequency from cloudsat ob-
 466 servations and the community earth system model. *The Cryosphere*, *14*(7),
 467 2253–2265.
- 468 Lingle, C. S., & Fatland, D. R. (2003). Does englacial water storage drive temperate
 469 glacier surges? *Annals of Glaciology*, *36*, 14–20.
- 470 Lupikasza, E. B., Ignatiuk, D., Grabiec, M., Cielecka-Nowak, K., Laska, M., Jania,
 471 J., ... Budzik, T. (2019). The role of winter rain in the glacial system on
 472 svalbard. *Water*, *11*(2), 334.
- 473 Mair, D., Nienow, P., Sharp, M., Wohlleben, T., & Willis, I. (2002). Influence of
 474 subglacial drainage system evolution on glacier surface motion: Haut glacier
 475 d’arolla, switzerland. *Journal of Geophysical Research: Solid Earth*, *107*(B8),
 476 EPM–8.
- 477 Mair, D., Willis, I., Fischer, U. H., Hubbard, B., Nienow, P., & Hubbard, A. (2003).
 478 Hydrological controls on patterns of surface, internal and basal motion during
 479 three “spring events”: Haut glacier d’arolla, switzerland. *Journal of Glaciol-*
 480 *ogy*, *49*(167), 555–567.
- 481 Mankoff, K. D., Gulley, J. D., Tulaczyk, S. M., Covington, M. D., Liu, X., Chen,
 482 Y., ... Głowacki, P. S. (2017). Roughness of a subglacial conduit un-
 483 der Hansbreen, Svalbard. *Journal of Glaciology*, *63*(239), 423–435. doi:

- 10.1017/jog.2016.134
- 484 Moore, G. (2016). The december 2015 north pole warming event and the increasing
 485 occurrence of such events. *Scientific Reports*, *6*(1), 1–11.
- 486 Müller, M., Homleid, M., Ivarsson, K.-I., Køltzow, M. A., Lindskog, M., Midtbø,
 487 K. H., ... others (2017). Arome-metcoop: A nordic convective-scale opera-
 488 tional weather prediction model. *Weather and Forecasting*, *32*(2), 609–627.
- 489 Nowak, A., & Hodson, A. (2013). Hydrological response of a high-arctic catchment
 490 to changing climate over the past 35 years: a case study of bayelva watershed,
 491 svalbard. *Polar Research*, *32*(1), 19691.
- 492 Oltmanns, M., Straneo, F., & Tedesco, M. (2019). Increased greenland melt trig-
 493 gered by large-scale, year-round cyclonic moisture intrusions. *The Cryosphere*,
 494 *13*(3), 815–825.
- 495 Pälli, A., Moore, J. C., Jania, J., Kolondra, L., & Glowacki, P. (2003). The drainage
 496 pattern of hansbreen and werenskioldbreen, two polythermal glaciers in sval-
 497 bard. *Polar Research*, *22*(2), 355–371.
- 498 Peeters, B., Pedersen, Å. Ø., Loe, L. E., Isaksen, K., Veiberg, V., Stien, A., ...
 499 Hansen, B. B. (2019). Spatiotemporal patterns of rain-on-snow and basal
 500 ice in high arctic svalbard: detection of a climate-cryosphere regime shift.
 501 *Environmental Research Letters*, *14*(1), 015002.
- 502 Pitcher, L. H., Smith, L. C., Gleason, C. J., Miège, C., Ryan, J. C., Hagedorn,
 503 B., ... Forster, R. R. (2020). Direct observation of winter meltwater
 504 drainage from the greenland ice sheet. *Geophysical Research Letters*, *47*(9),
 505 e2019GL086521.
- 506 Schoof, C. (2010). Ice-sheet acceleration driven by melt supply variability. *Nature*,
 507 *468*(7325), 803–806.
- 508 Schoof, C., Rada, C., Wilson, N., Flowers, G., & Haseloff, M. (2014). Oscillatory
 509 subglacial drainage in the absence of surface melt. *The Cryosphere*, *8*(3), 959–
 510 976.
- 511 Schroeder, J. (1998a). Hans glacier moulines observed from 1988 to 1992, svalbard.
 512 *Norwegian Journal of Geography*, *52*(2), 78–88.
- 513 Schroeder, J. (1998b). Indications of climate change from moulin evolution.
 514 *Salzburger Geographische Materialien*, *28*, 27–33.
- 515 Schroeder, J. (2007). Moulines of a subpolar glacier seen as a thermal anomaly. In
 516 *Karst and cryokarst: Joint proceedings of the 25th speleological school and 8th*
 517 *international glackipr symposium* (pp. 65–74).
- 518 Screen, J. A., & Simmonds, I. (2012). Declining summer snowfall in the arctic:
 519 Causes, impacts and feedbacks. *Climate dynamics*, *38*(11-12), 2243–2256.
- 520 Sobota, I., Weckwerth, P., & Grajewski, T. (2020). Rain-on-snow (ros) events and
 521 their relations to snowpack and ice layer changes on small glaciers in svalbard,
 522 the high arctic. *Journal of Hydrology*, *590*, 125279.
- 523 Sole, A., Nienow, P., Bartholomew, I., Mair, D., Cowton, T., Tedstone, A., & King,
 524 M. A. (2013). Winter motion mediates dynamic response of the greenland ice
 525 sheet to warmer summers. *Geophysical Research Letters*, *40*(15), 3940–3944.
- 526 Stevens, L. A., Behn, M. D., Das, S. B., Joughin, I., Noël, B. P., van den Broeke,
 527 M. R., & Herring, T. (2016). Greenland ice sheet flow response to runoff
 528 variability. *Geophysical Research Letters*, *43*(21), 11–295.
- 529 Sund, M., Lauknes, T. R., & Eiken, T. (2014). Surge dynamics in the nathorstbreen
 530 glacier system, svalbard. *The Cryosphere*, *8*(2), 623–638.
- 531 Turu, V. (2012). Surface nmr survey on hansbreen glacier, hornsund, sw spitsbergen
 532 (norway). *Landform Analysis*, *21*, 57–74.
- 533 Vieli, A., Jania, J., Blatter, H., & Funk, M. (2004). Short-term velocity varia-
 534 tions on hansbreen, a tidewater glacier in spitsbergen. *Journal of Glaciology*,
 535 *50*(170), 389–398.
- 536 Vijay, S., Khan, S. A., Kusk, A., Solgaard, A. M., Moon, T., & Bjørk, A. A. (2019).
 537 Resolving seasonal ice velocity of 45 greenlandic glaciers with very high tempo-
 538

- 539 ral details. *Geophysical Research Letters*, *46*(3), 1485–1495.
- 540 Vikhamar-Schuler, D., Isaksen, K., Haugen, J. E., Tømmervik, H., Luks, B., Schuler,
541 T. V., & Bjerke, J. W. (2016). Changes in winter warming events in the nordic
542 arctic region. *Journal of climate*, *29*(17), 6223–6244.
- 543 Wadham, J., Tranter, M., & Dowdeswell, J. (2000). Hydrochemistry of meltwaters
544 draining a polythermal-based, high-arctic glacier, south svalbard: Ii. winter
545 and early spring. *Hydrological Processes*, *14*(10), 1767–1786.
- 546 Werder, M. A., Hewitt, I. J., Schoof, C. G., & Flowers, G. E. (2013). Modeling chan-
547 nelized and distributed subglacial drainage in two dimensions. *Journal of Geo-*
548 *physical Research: Earth Surface*, *118*(4), 2140–2158.
- 549 Willis, I. C. (1995). Intra-annual variations in glacier motion: a review. *Progress in*
550 *Physical Geography*, *19*(1), 61–106.
- 551 Winsvold, S. H., Kääh, A., Nuth, C., Andreassen, L. M., Van Pelt, W. J., & Schel-
552 lenberger, T. (2018). Using sar satellite data time series for regional glacier
553 mapping. *The Cryosphere*, *12*(3), 867–890.
- 554 Wu, B. (2017). Winter atmospheric circulation anomaly associated with recent arctic
555 winter warm anomalies. *Journal of Climate*, *30*(21), 8469–8479.